EMI Camera LSI (EMcam) with 12 x 4 On-Chip Loop Antenna Matrix in 65-nm CMOS to Measure EMI Noise Distribution with 60-μm Spatial Precision

Naoki Masunaga, Koichi Ishida, Makoto Takamiya, and Takayasu Sakurai

University of Tokyo, 4-6-1 Komaba, Meguro-ku, Tokyo 153-8505, Japan

Abstract- **An EMI Camera LSI (EMcam) with a 12 x 4 on-chip 250μm x 50μm loop antenna matrix in 65nm CMOS is developed. EMcam achieves both the 2D electric scanning and 60μm-level spatial precision for the first time. The down-conversion architecture increases the bandwidth of EMcam and enables the measurement of EMI spectrum. Shared IF block scheme is proposed to alleviate the increasing power and area penalty inherent to the matrix measurement. 'Mixer and antenna selector (MAS)' reduces the switches and prevents the EMI attenuation due to the switches. EMI measurement with the smallest 32μm x 12μm antenna to date is also demonstrated.**

I. INTRODUCTION

An EMI in electronic devices such as cell-phones is becoming a serious problem because of (1) the increasing density of the packaging, (2) the increasing number of various RF transceivers within a electronic device, and (3) the increasing signal frequency (>1GHz) which result in the downsizing of the EMI antenna. In order to measure the EMI noise generated from the fine pattern on PCB or the on-chip interconnect, 2D EMI distribution measurement with 60μm-level spatial precision is required. To efficiently and accurately measure the 2D EMI distribution, the electric scanning instead of the conventional mechanical scanning of the EMI probe [1] is required. All the conventional measurement method, however, do not satisfy both the 2D electric scanning and the 60-μm precision. The spatial precision of the conventional 2D electric scanning [2-4] is more than 7.5mm. Though the smallest EMI probe with 50μm x 22μm is reported [5], the probe is single and used for the mechanical scanning.
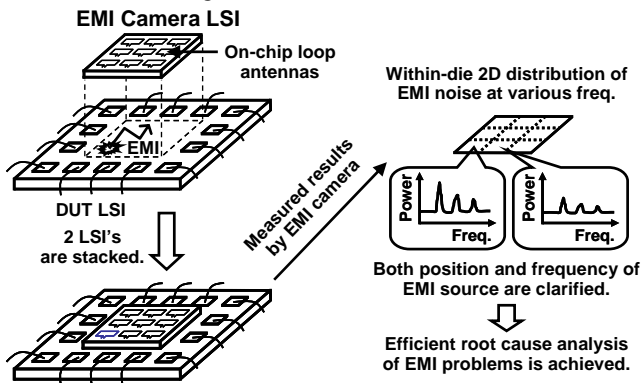
To solve the problem of the conventional EMI measurement methods, an EMI camera LSI (EMcam) with the matrix of on-chip loop antennas and measurement circuits is proposed. By using the EMcam, 2D EMI distribution measurement with 60μm-level spatial precision is demonstrated for the first time.

II. EMI CAMERA LSI (EMCAM)

Fig. 1 shows an overview and benefits of the proposed EMcam. By putting the EMcam on top of a DUT LSI, the EMcam measures within-die 2D distributions of EMI noise at various frequencies. By clarifying the position and the frequency of the EMI source, an efficient root cause analysis of the EMI problems is achieved, because the EMI frequency is an important clue to find the EMI source.

Fig. 2 shows a block diagram of the measurement core circuit in the EMcam. The EMI noise is picked up by the on-chip loop antenna. Then the noise inputs are down-converted, amplified, and low-pass-filtered. While the noise inputs are just amplified by high-bandwidth amplifiers in [6], the down-conversion is very important in our matrix measurement, because the down-converted noise can be handled with the low-bandwidth amplifiers consuming low power, which
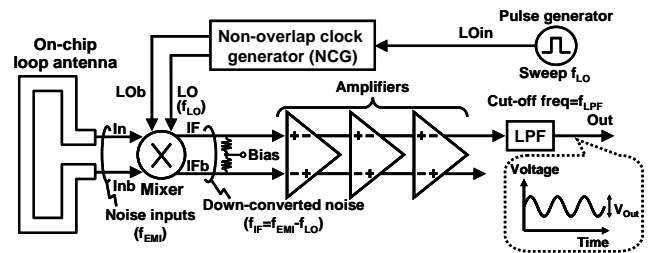

Fig. 2. Block diagram of measurement core circuit in EMcam.

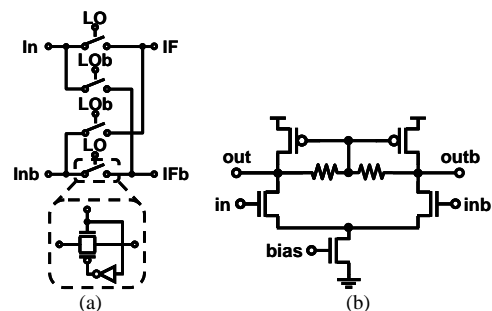Fig. 1. Overview and benefits of the proposed EMI camera.

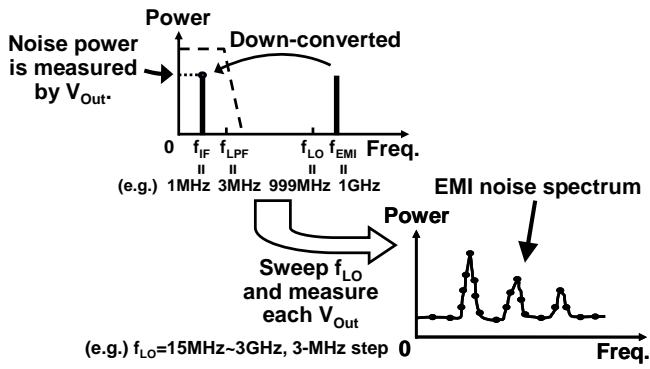Fig. 3. Circuit schematics. (a) Mixer. (b) Amplifier.

Fig. 4. Procedure to obtain EMI noise spectrum using the circuit in Fig. 2.

reduces power and increases the bandwidth of EMcam. Fig. 3 shows schematics of the mixer and the amplifier in Fig. 2. The passive mixer is used to reduce the power. The amplifier is a differential amplifier with the common mode feedback. Fig. 4 shows a procedure to obtain the EMI noise spectrum using the circuit in Fig. 2. By sweeping f_{LO} and measuring V_{Out} shown in Fig. 2 at each f_{LO}, the EMI noise spectrum is obtained.

Figs. 5 (a) and (b) show schematics of the straightforward and proposed measurement circuit array in the EMcam, respectively. 4 measurement units are shown. In order to alleviate the increasing power and area penalty inherent to the matrix measurement, the IF block is shared between 4 antennas. Each antenna has the mixer and the non-overlap clock generator (NCG). The analog signal (Out) is converted to a digital signal by a rectifier and a comparator. In the
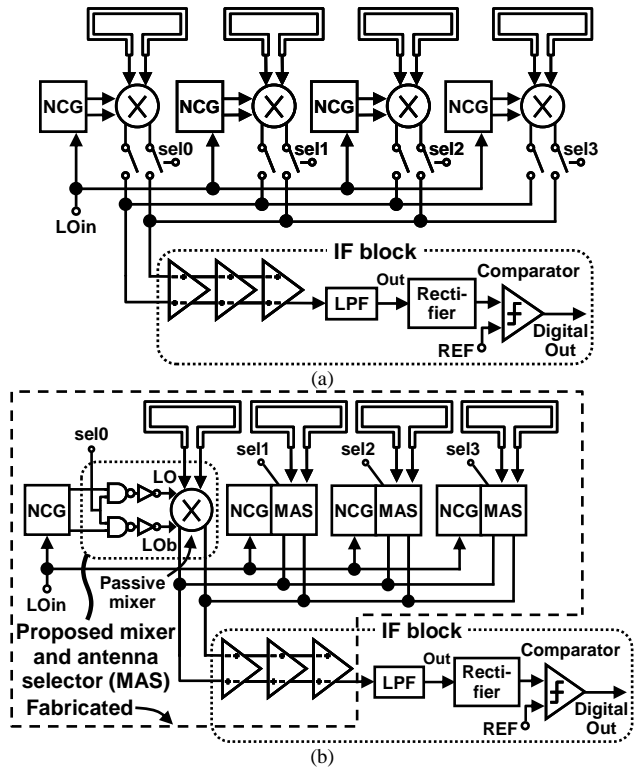

Fig. 5. Schematic of (a) straightforward and (b) proposed measurement circuit array in EMcam.
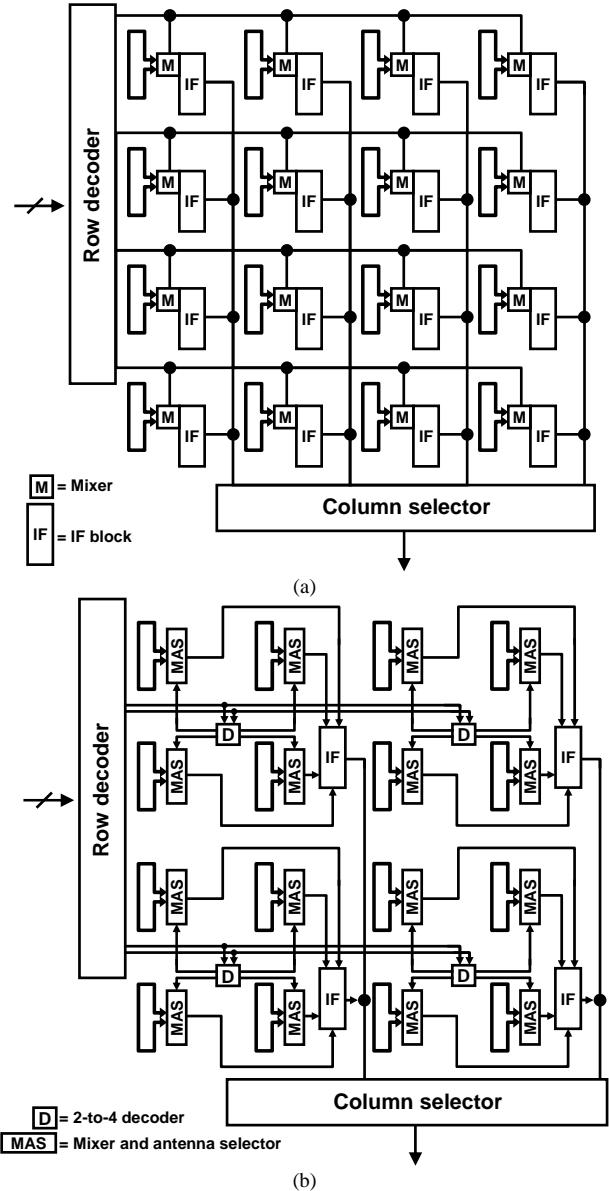

(a)

(b)

Fig. 6. Schematic of (a) straightforward and (b) proposed matrix circuits in EMcam.

straightforward circuit array (Fig. 5(a)), switches are inserted between the mixer and the IF block. The switches attenuate the measured EMI noise and the sensitivity of the measurement circuit is degraded. In contrast, in the proposed circuit array (Fig. 5(b)), each antenna has the proposed 'mixer and antenna selector (MAS)'. When sel0 is high, MAS operates as the mixer. When sel0 is low, both LO and LOb are low, and the antenna is separated from the amplifiers. Because the proposed MAS can operate as both the mixer and antenna selector, the additional switches in Fig. 5(a) are not required and the attenuation due to the additional switches is avoided.

Fig. 6 shows a schematic of the straightforward and proposed matrix circuits in the EMcam. In the straightforward matrix, each antenna has the mixer and the IF block. In contrast, in the proposed matrix, each antenna has MAS, and 4
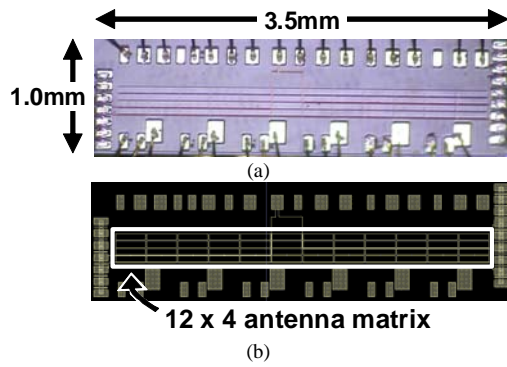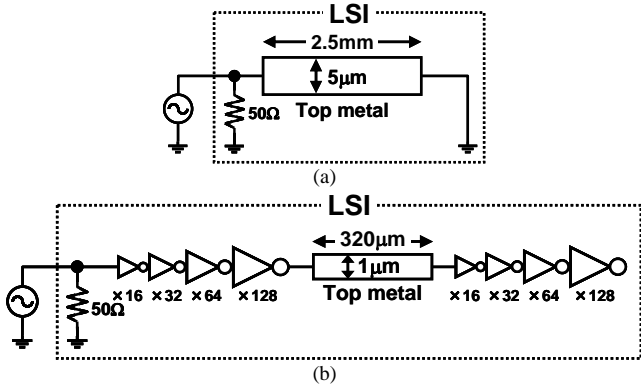
Fig. 7. (a) Chip micrograph. (b) Layout.

Fig. 8. On-chip DUT's for EMI generation. (a) DUT (wire). (b) DUT (buffer).

antennas share a decoder and the IF block. By sharing the high-power IF block, the power and the circuit area are reduced by 74% and 73%, respectively.

III. EXPERIMENTAL RESULTS

The front-end block of the EMcam shown in Fig. 5 (b) was fabricated in 1.2V, 65nm CMOS process. The chip micrograph and layout are shown in Fig. 7 and the performance is summarized in Table I. A 12 x 4 on-chip loop antenna matrix is embedded and the size of the antenna is 250μm x 50μm. In order to check the performance of the EMcam without using the 2 stacked chips, DUT's are also embedded on the same chip. Fig. 8 shows a schematic of the
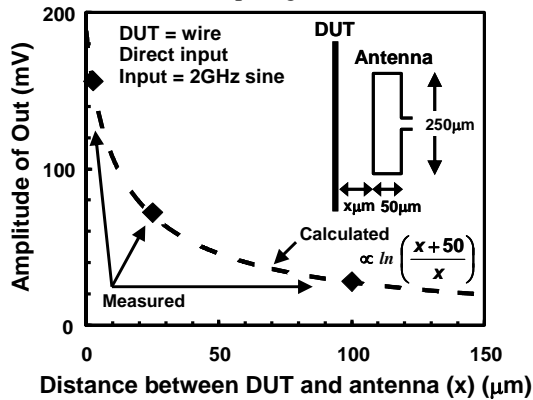

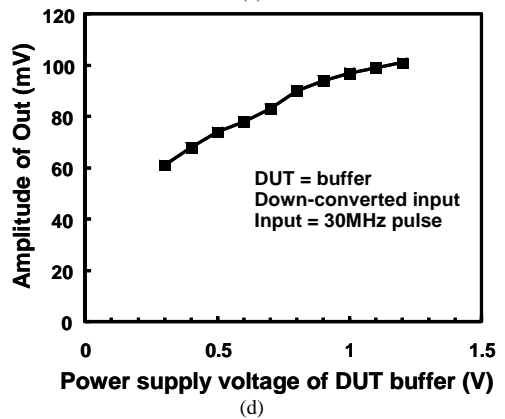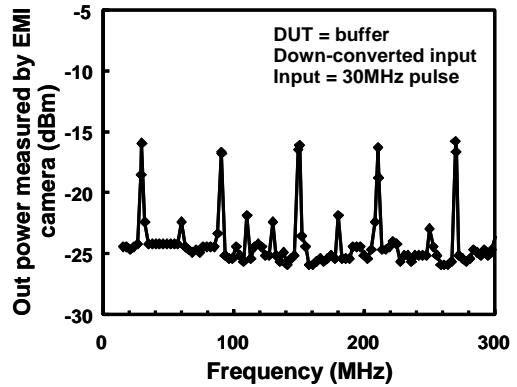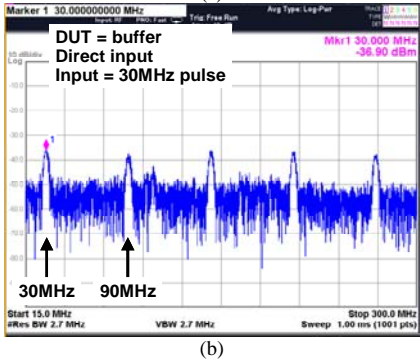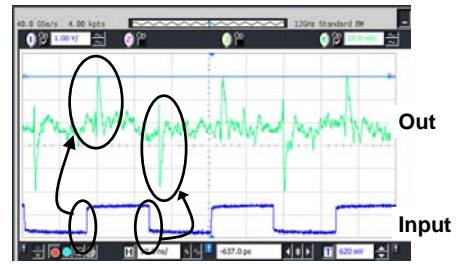Fig. 9. Measured and calculated dependence of EMcam output on the distance between DUT (wire) and antenna.

Fig. 10. EMI noise of DUT (buffer). (a) Noise waveform. (b) Noise spectrum for reference. (c) Noise spectrum using the EMcam. (d) Measured dependence of EMcam output on power supply voltage of DUT.

two DUT's for EMI generation. In the DUT (wire), a long on-chip wire is driven by an off-chip signal generator. The DUT (buffer) emulates clock buffers for global clock distribution.

Fig. 9 shows a measured and calculated dependence of the amplitude of the EMcam output on the distance between the
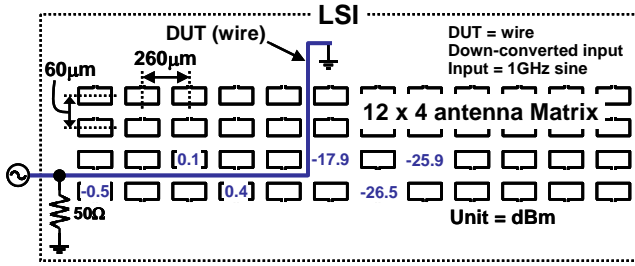
Fig. 11. Within-die 2D distribution of EMI noise measured with the 12 x 4 on-chip antenna matrix.
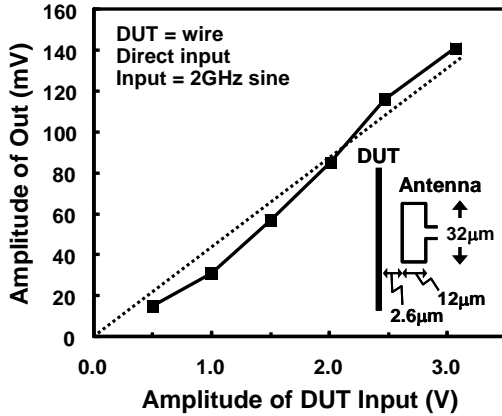
Fig. 12. Measured dependence of EMcam output on DUT (wire) input with the smallest antenna.

TABLE I PERFORMANCE SUMMARY.

Technology		65nm CMOS
Supply voltage		1.2V
EMI camera LSI	Gain	47dB
	Maximum frequency	3.3GHz
	Frequency resolution	3MHz
	Dynamic range	33dB
On-chip loop antenna	Number	12 x 4 array
	Size	250μm x 50μm (array) 32μm x 12μm (single)
	Antenna pitch	60μm (vertical) 260μm (horizontal)
Power	Amplifiers	16.06mW
	MAS and NCG	0.16mW
	Total	16.22mW
Core area	Amplifiers	2130μm²
	MAS and NCG	46μm²
	Total	2176μm²

DUT (wire) and the antenna. In this measurement, the NCG is turned off and the noise inputs are not down-converted and directly measured. The measured results are consistent with the calculated results, which confirm the validity of the EMcam. The EMI noise generated by the DUT (buffer) is evaluated, because the clock buffer is the main EMI source in an LSI. Figs. 10 (a) and (b) show measured EMI noise waveform and spectrum of DUT (buffer) using the off-chip oscilloscope and spectrum analyzer, respectively. The NCG is turned off, similar to Fig. 9. In Fig. 10 (a), the EMI noise waveform is clearly shown at the rising and falling edge of the 30-MHz clock signal. Fig. 10 (c) shows corresponding EMI noise spectrum measured with the EMcam. In Figs. 10 (b) and (c), the noise peaks match, which confirms the validity of the EMcam. Fig. 10 (d) shows a measured dependence of the amplitude of the EMcam output on the power supply voltage of the DUT (buffer). The amplitude is reduced with the reduced power supply voltage, because the EMI noise generation is reduced. Fig. 11 shows a within-die 2D distribution of EMI noise measured with the 12 x 4 on-chip loop antenna matrix of the EMcam. The antenna pitch is 60μm and 260μm in a vertical and horizontal direction, respectively. The DUT wire goes across the matrix. As the distance between the DUT and the antenna increases, the measured EMI noise decreases.

In order to show the feasibility of the more precise EMcam, EMI measurement with the smallest size loop antenna (32μm x 12μm) to date is demonstrated. Fig. 12 shows a measured dependence of the amplitude of the EMcam output on the amplitude of the DUT (wire) input. As the input amplitude decreases, the output amplitude linearly decreases, which shows a reasonable operation of the smallest antenna.

IV. CONCLUSION

An EMI Camera LSI with a 12 x 4 on-chip 250μm x 50μm loop antenna matrix in 65 nm CMOS is developed. Without mechanical scanning, within-die 2-D distribution of EMI noise is measured for the first time at 60-μm-level spatial precision. The down-conversion architecture increases the bandwidth of EMcam and enables the measurement of EMI spectrum. Shared IF block architecture reduced the power and the area by 74% and 73%, respectively. 'Mixer and antenna selector (MAS)' reduces the switches and prevents the EMI attenuation due to the switches. EMI measurement with the smallest 32μm x 12μm antenna to date is also demonstrated.

ACKNOWLEDGMENTS

REFERENCES

[1] Magnetic field probe (CP-1S), NEC Corporations.
[2] EMSCAN. [Online]. Available: http://emscan.com/
[3] K. Ishida, N. Masunaga, Z. Zhou, T. Yasufuku, T. Sekitani, U. Zschieschang, H. Klauk, M. Takamiya, T. Someya, and T. Sakurai, "Stretchable EMI Measurement Sheet With 8 X 8 Coil Array, 2 V Organic CMOS Decoder, and 0.18 um Silicon CMOS LSIs for Electric and Magnetic Field Detection," IEEE Journal of Solid-State Circuits, Vol. 45, No. 1, pp. 249-259, Jan. 2010.
[4] N. Masunaga, K. Ishida, Z. Zhou, T. Yasufuku, T. Sekitani, T. Someya, M. Takamiya, and T. Sakurai, "A Flexible EMI Measurement Sheet to Measure Electric and Magnetic Fields Separately with Distributed Antennas and LSI's," IEEE International Symposium on Electromagnetic Compatibility, pp. 156-160, Aug. 2009.
[5] N. Ando, N. Masuda, N. Tarnaki, T. Kuriyama, S. Saito, K. Kato, K. Ohashi, M. Saito, M. Yarnaguchi, "Miniaturized thin-film magnetic field probe with high spatial resolution for LSI chip measurement," IEEE International Symposium on Electromagnetic Compatibility, vol. 2, pp. 357-362, Aug. 2004.
[6] S. Aoyama, S. Kawahito, M. Yamaguchi, "An Active Magnetic Probe Array for the Multiple-Point Concurrent Measurement of Electromagnetic Emissions," IEEE Trans. Magn., vol. 42, no. 10, pp. 3303-3305, Oct. 2006.